Joint impact on thermotolerance of *Saccharomyces* species divergence in mitochondrial and nuclear genomes

Jun-Ting Johnson Wang[1,2], Ping Ling Priscilla Ng[1,3], Maceo E. Powers[1,4], Rachel B. Brem[1*]

[1]Department of Plant and Microbial Biology, University of California, Berkeley, Berkeley, CA, 94720

[2]Graduate Group in Comparative Biochemistry, University of California, Berkeley, Berkeley, CA, 94720

[3]Current address: BillionToOne, Menlo Park, CA, 94025

[4]Current address: Laboratory of Viral Diseases, National Institute of Allergy and Infectious Diseases, National Institutes of Health, Bethesda, MD, 20892

*To whom correspondence should be addressed (rbrem@berkeley.edu)

Keywords: Trait variation, evolution, mitochondrial divergence, positive epistasis

Abstract

Many traits of interest in biology evolved long ago and are fixed in a particular species, distinguishing it from other sister taxa. Elucidating the mechanisms underlying such ancient traits has been a central goal for evolutionary biologists. The yeast *Saccharomyces cerevisiae* is unique among its relatives for its ability to thrive at high temperature, via a genetic architecture that remains incompletely understood. We sought to understand the contribution of species variation in mitochondrial DNA to yeast thermotolerance. We used mitochondrial transgenesis to show that *S. cerevisiae* mitotypes were sufficient for a partial boost to thermotolerance and respiration in the *S. paradoxus* background. These mitochondrial alleles worked best when the background also harbored a pro-thermotolerance nuclear genotype, attesting to positive epistasis between the two genomes. The benefits of *S. cerevisiae* alleles in terms of respiration and growth at high temperature came at the cost of worse performance in cooler conditions. Together, our results establish this system as a case in which mitoalleles have fitness benefits and work well in multiple backgrounds; given the high mutation rate of the mitochondrial compartment, they were also likely extra easy for the ancestral population to acquire. We thus propose a broader model in which mitochondrial variants may prove to be especially good candidates in the search for genetic mechanisms of the adaptive process.

Introduction

A central aim in evolutionary genetics is to figure out how organisms acquire new traits. In the study of within-species variation, a rich literature has provided insights into the mechanisms of local adaptation in the wild (Elena 2017; Kraemer and Boynton 2017; Sork 2017; Rees et al. 2020; Bazzicalupo 2022). Yet many characters of basic and applied interest evolved long ago and are fixed in a particular species, distinguishing it from unaffected relatives. Against a backdrop of years of genomic and experimental pursuit (Allen Orr 2001; Nikolov and Tsiantis 2015; Weiss and Brem 2019), as a field we still know surprisingly little about how evolution engineers and refines phenotypes over long timescales, with the widest knowledge gap in the case of polygenic architectures. Shedding light on these processes, by dissecting the genetics of ancient traits, remains a key challenge for the field.

Sequence variants in mitotype, the DNA of the mitochondrial organelle, have emerged as an important part of the genetic architecture of naturally varying traits. Mitotype variants have been directly implicated in trait innovation, both independently and in concert with nuclear genomes (Melvin and Ballard 2006; Tranah 2011; Houtkooper et al. 2013; Sullivan and Chandel 2014; Sun et al. 2019; Cao et al. 2022; Meng et al. 2022; Oppong et al. 2022; Quéméneur et al. 2022; Parra et al. 2023; Moran et al. 2024). Though small in length, the mitochondrial genome has the potential for an outsize influence on trait variation, given its increased mutation rate and large mutational target of the multi-copy mitochondrial genome relative to nuclear chromosomes (Pakendorf and Stoneking 2005; Chou and Leu 2015; Ferreira and Rodriguez 2024).

Saccharomyces budding yeasts diverged from a common ancestor ~20 million years ago (Kellis et al. 2003) and have served for decades as a model for the study of interspecific trait variation, including in metabolism, genome content, cell cycle, and reproductive isolation (Hou et al. 2014; Roop et al. 2016; Bozdag et al. 2021; Fredericks et al. 2021; Lupo et al. 2021; Marsit et al. 2021; Smukowski Heil et al. 2021; Swamy et al. 2022; Crandall et al. 2023; Forejt and Jansa 2023; Peris et al. 2023). A long-standing subset of this field has focused on species-unique traits driven by mitochondrial genomes (Sulo et al. 2003; Wolff et al. 2014; De Chiara et al. 2020; Hewitt et al. 2020; Hénault et al. 2022), with particularly detailed mechanistic validation in studies of speciation (Lee et al. 2008; Chou et al. 2010; Mário et al. 2015; Jhuang et al. 2017). Such findings from ancient traits serve as a complement to studies of within-species mitotype

variation in yeast (Wolters et al. 2015; Leducq et al. 2017; Wolters et al. 2018; Vijayraghavan et al. 2019; Vijayraghavan et al. 2019; Nguyen et al. 2020). A key model for ancient trait variation in the *Saccharomyces* system is temperature response, as the best-studied yeast species, *S. cerevisiae,* is unique within the *Saccharomyces* clade for its ability to thrive at high temperature (Sweeney et al. 2004; Gonçalves et al. 2011; Salvadó et al. 2011), whereas others in the clade exhibit cryotolerance (Paget et al. 2014; Pinto et al. 2025). A growing literature has implicated nuclear loci in species differences in thermotolerance (Weiss et al. 2018; AlZaben et al. 2021; Walunjkar et al. 2024) and cold tolerance (Paget et al. 2014; Pinto et al. 2025). The contribution of mitochondrial genome variation to this trait has also been suggested, based on analyses of interspecies hybrids (Baker et al. 2019; Li et al. 2019; Hewitt et al. 2020); exactly what the divergent mitotypes of *Saccharomyces* species do phenotypically, and how they exert their effects, remains incompletely understood.

We set out to deepen our understanding of the phenotypic impact of mitochondrial variation between *Saccharomyces* species, both in isolation and in conjunction with nuclear loci. We anticipated that our findings would further illuminate the mechanisms of thermotolerance and their evolutionary history. We designed an approach that used *S. paradoxus*, a relatively thermosensitive species sister to *S. cerevisiae,* as a model for the common ancestor on whose background traits would have arisen as the two species diverged. We manipulated the nuclear and mitochondrial genome in this system to investigate their contributions to metabolism and thermotolerance.

Results

S. cerevisiae* mitotypes are sufficient to heighten respiratory behaviors in *S. paradoxus

Previous studies have used yeast interspecies hybrids to establish an association between *S. cerevisiae* mitochondrial alleles and thermotolerance (Baker et al. 2019; Li et al. 2019; Hewitt et al. 2020), which parallels the advantage of *S. cerevisiae* purebreds at high temperature, relative to other species in the clade. We reasoned that investigating mitotype genetics in purebred *S. paradoxus* could help shed additional light on the mechanisms of evolutionary innovation along the *S. cerevisiae* lineage. For this purpose, we developed a series of cybrids (cytoplasmic hybrids), in which we introduced each mitochondrial genome in turn from a suite of *S. cerevisiae* isolates from different geographical locations, which all grew well in standard conditions and at high temperature (Figure S1), into a tester strain of *S. paradoxus*, the English oak tree isolate Z1 (Figure 1). Since they lack the endogenous *S. paradoxus* mitotype, these strains represented an experimental resource for the study of the phenotypic impact of *S. cerevisiae* mitochondrial alleles in an isogenic background, and they were viable and stable as expected (Sulo et al. 2003; Mário et al. 2015).

Before using our cybrids to address thermotolerance *per se*, we first investigated the hypothesis that respiration, as a proximal function of the mitochondrion and its genome, would be perturbed by species variation in mitotype. Wild-type *S. cerevisiae* strains as a rule grow better than those of *S. paradoxus* on glycerol, a non-fermentable carbon source (Figure S2), and in interspecies hybrid backgrounds, *S. cerevisiae* mitotypes promote growth in this condition (Li et al. 2019). To explore the impact of *S. cerevisiae* mitochondrial DNA alleles on respiratory growth in a purebred context, we subjected our cybrids to the liquid growth assay in glycerol media. The results revealed robust improvement in glycerol growth attributable to *S. cerevisiae* mitotypes in the *S. paradoxus* background, for three of our *S. cerevisiae* donors (Figure 2A). The fourth cybrid, harboring mitochondrial DNA from the *S. cerevisiae* vineyard isolate Y55, had a defect in growth on glycerol (Figure 2A), which echoes previously reported incompatibilities of this mitotype in other backgrounds (Wolters et al. 2018). Together, these data suggested that pro-

respiratory effects could be a prevalent characteristic of mitochondrial genomes from across the *S. cerevisiae* population.

As a more direct measure of metabolic effects driven by *S. cerevisiae* mitochondria DNA, we established an assay of reduction of the colorimetric substrate 1-(4,5-dimethylthiazol-2-yl)-3,5-diphenyltetrazolium bromide (MTT) in glucose medium. This signal serves as a reporter of activities of the electron transport chain, particularly succinate dehydrogenase (Slater et al. 1963; Sánchez and Königsberg 2006; Jain et al. 2018) (though see (Shoemaker et al. 2004) and (Peng et al. 2005)), and thus is informative as a marker of respiration. A first set of observations revealed no detectable impact of mitotype on MTT reduction during culture in liquid glucose medium at 28°C, in our cybrids in the Z1 *S. paradoxus* background (Figure 3A). We reasoned that the metabolic effect of *S. cerevisiae* mitotypes might be better resolved at higher temperatures, in which yeast cells respire more avidly (Rikhvanov et al. 2001). Consistent with this notion, in culture at 39°C in glucose medium, we observed increased MTT reduction in all cybrids except for that harboring *S. cerevisiae* Y55 mitochondrial DNA, relative to wild-type Z1 *S. paradoxus* with its endogenous mitochondrial genome (Figure 3B). Together, these results established that in the *S. paradoxus* background, *S. cerevisiae* mitotypes can be sufficient for increased growth and metabolic behaviors that are signatures of respiration.

S. cerevisiae* mitotypes boost thermotolerance in *S. paradoxus

We now turned to high-temperature growth proper, as an additional phenotype that we hypothesized would be modulated by mitotype in our yeast species comparison. To test the latter prediction, we measured carrying capacity during growth in liquid glucose medium at 39°C, for each of our cybrid strains harboring *S. cerevisiae* mitochondrial DNA in Z1 *S. paradoxus*. Results revealed a 10% to 70% improvement in accumulated biomass in this assay, relative to wild-type *S. paradoxus,* in all cybrids except the one for which *S. cerevisiae* Y55 was the mitochondrial donor (Figure 2A). Thus, *S. cerevisiae* mitotypes were sufficient to confer thermotolerance benefits, in some cases sizeable ones, in *S. paradoxus*. After 24 hours of incubation at 39°C, only *S. cerevisiae* wild-type cells retained viability, whereas cultures of all strains in the *S. paradoxus* background harbored very few viable cells (Figure S3). We conclude that in our cybrids, *S. cerevisiae* mitochondrial DNAs enable additional cell divisions during high-temperature exposure, though failures of factors encoded by the *S. paradoxus* nuclear genome ultimately prevent further growth and kill cells outright.

Thermotolerance phenotypes as they varied across our panel of strains correlated tightly with the respiratory behaviors we had documented in assays of growth in the non-fermentable carbon source glycerol (Figures 2A and 2B) and of MTT reduction (Figure 3). That is, among our strains, those performing best in respiratory contexts were the most thermotolerant, and the worst in respiratory assays grew the worst at high temperature. These results are most consistent with a causal relationship between the traits, whereby the *S. cerevisiae* mitotypes that foster better thermotolerance do it by improving respiration—a metabolic underpinning for the capacity to grow under high-temperature challenge.

Antagonistic pleiotropy by *S. cerevisiae* mitotypes in temperate conditions and ethanol

Previous studies using interspecies hybrids have reported a defect in cold temperatures attributable to *S. cerevisiae* mitotypes relative to those of *S. paradoxus* or other relatives (Baker et al. 2019; Li et al. 2019; Hewitt et al. 2020). To test whether such effects would be recapitulated in purebred backgrounds, for each of our Z1 *S. paradoxus* derivatives carrying *S. cerevisiae* mitochondrial DNA, we assayed the carrying capacity after culture 23°C in liquid glucose medium, for comparison against a 28°C control and the high-temperature condition (39°C), also with glucose as a carbon source. The results revealed compromised carrying

capacity at the lower temperatures in the cybrids that performed the best at high temperature (Figure 2A). This set up an almost perfect anticorrelation between the growth patterns of high and moderate temperatures across strains (Figure 2C), mirroring the observation we had made with respiratory behaviors (Figures 2 and 3). Interestingly, a similar principle held true in assays using ethanol as the carbon source, where again the least thermotolerant strains grew the best (Figures 2A and 2D). Together, our growth and respiration data make clear that *S. cerevisiae* mitotypes have specialized to heat stress at the expense of performance at lower temperatures and during ethanol utilization.

Positive epistasis between mitochondria and nuclear genomes in terms of thermotolerance

During the evolution of *S. cerevisiae* as a species, the pro-thermotolerance mitotypes we study here would have arisen alongside changes in nuclear genes which could modify their effects. We sought to shed light on these relationships by modeling them in the *S. paradoxus* background. To this end, we introduced *S. cerevisiae* mitochondrial genomes into a derivative of *S. paradoxus* Z1 that also harbored nuclear alleles from the DBVPG1373 Dutch soil strain of *S. cerevisiae,* at eight loci which contribute to thermotolerance (*AFG2, APC1, CEP3, DYN1, ESP1, MYO1, SCC2*, and *TAF2*, most of which encode cell division factors; (AlZaben et al. 2021)). In assays of carrying capacity at 39°C, the combination of *S. cerevisiae* alleles in the nuclear and mitochondrial genomes together conferred a two-fold improvement relative to wild-type *S. paradoxus* (Figure 4, squares). No such effect was detectable in 28°C cultures (Figure S4). This represented an increase in cell divisions early in the treatment, as no cybrids harboring *S. cerevisiae* nuclear alleles maintained viability after 24 hours at 39°C (Figure S5), paralleling results from cybrids in the wild-type *S. paradoxus* nuclear background (Figure S3). Advantages in carrying capacity at 39°C manifested regardless of the origin of the mitotype: mitochondrial DNA from each of the four *S. cerevisiae* strain donors yielded identical high-temperature growth in *S. paradoxus* in the presence of the nuclear thermotolerance genes from *S. cerevisiae,* including the Y55 mitotype that had compromised the phenotype in wild-type *S. paradoxus* (Figures 2A and 4). Thus, the latter incompatibility was resolved by *S. cerevisiae* alleles at our focal nuclear genes.

Also evident from our nuclear-mitochondrial transgenic strain panel was a pattern of positive epistasis. That is, the impact of each *S. cerevisiae* mitotype on thermotolerance was greater in the *S. paradoxus* derivative also harboring nuclear alleles from *S. cerevisiae* than in otherwise wild-type *S. paradoxus* (Figure 4; compare circles and squares). No such dependence was detectable at 28°C (Figure S4). Thus, mitochondrial DNA from distinct *S. cerevisiae* donors, including Y55, all achieved peak performance at high temperature in the presence of *S. cerevisiae* nuclear genes. This effect did not reach significance for the *S. cerevisiae* mitotype that promoted thermotolerance most strongly on its own in the *S. paradoxus* background, from DBVPG1373; it benefited the least from the addition of DBVPG1373 alleles of nuclear genes (Figure 4, magenta). Relative to this transgenic, strains harboring other *S. cerevisiae* mitotypes, which had less impact on their own, achieved the same carrying capacity at 39°C in the presence of DBVPG1373 nuclear alleles (Figure 4, blue, green, and orange). These results are most consistent with a ceiling beyond which any *S. cerevisiae* alleles of the mitochondrial genome, even when combined with *S. cerevisiae* alleles of our eight focal nuclear genes, are unable to improve thermotolerance, in the face of defects accruing from other *S. paradoxus* loci. Nonetheless, our data make clear that pro-thermotolerance alleles of mitochondrial DNAs and nuclear genes from *S. cerevisiae* together contribute to the phenotype in a manner that exceeds the sum of their parts.

Discussion

A key goal of comparative genetics is to understand how evolution builds traits over long timescales. In this work, we have leveraged tractable *Saccharomyces* as a testbed for the study of interspecies trait genetics and evolution focused on the mitochondrial genome. Given the evidence that *S. cerevisiae* thermotolerance is the product of positive selection (Weiss et al. 2018; Abrams et al. 2021), it serves as a useful model of the evolutionary genetics of adaptation over deep divergences. Our findings complement previous studies of mitotype effects in this system in interspecies hybrids (Baker et al. 2019; Li et al. 2019; Hewitt et al. 2020) by tracing the phenotypes conferred by *S. cerevisiae* mitochondrial alleles in purebred backgrounds, including their genetic dependencies.

Our results shed new light on the genetic architecture and evolution of thermotolerance. Our finding of a 70% boost in the trait by an *S. cerevisiae* mitotype outstrips the effect of any one of the nuclear loci previously reported in this system (Weiss et al. 2018). That said, not all *S. cerevisiae* mitotypes had a benefit of this magnitude, as might be expected given the extensive precedent for polymorphism among mitochondrial genomes and their effects on human disease (Wallace 2015) as well as traits in animals (Tsai and St. John 2016; Brand et al. 2024; Serrano et al. 2024) and plants (Dubrovina and Kiselev 2016; Adhikari et al. 2019; Jo et al. 2019). Some of the *S. cerevisiae* mitotypes we study here could be ancient, if each was part of a soft selective sweep in the ancestral population when the trait arose, of the kind reported recently in a plant selfing system (Bergero et al. 2019). Perhaps more plausibly, *S. cerevisiae* mitochondrial polymorphisms could be the product of recent mutations on a background that underwent a hard sweep long ago.

Our data also make clear that alongside largely beneficial marginal effects, all *S. cerevisiae* mitotypes are even more advantageous at high temperature in the context of pro-thermotolerance nuclear alleles. To date, such evidence for positive epistasis has been at a premium in the literature describing adaptive loci from the wild (Nelson and Grishin 2018; Syenina et al. 2020; Stern et al. 2022). This may be in part owing to a heavier emphasis in the field on the evolutionarily difficult repacking of a given protein interior to achieve fitness (Weinreich et al. 2005; Starr and Thornton 2016), which could be more constrained than combinations of adaptive alleles of multiple proteins. But even the unlinked nuclear genes underlying S*. cerevisiae* thermotolerance do not exhibit positive epistasis among themselves (though their combinations do boost the trait; AlZaben et al. 2021). As such, our data point to mitoalleles, during the evolution of *S. cerevisiae* thermotolerance, as candidate cases of especially easily accessible (Liao et al. 2022) and highly beneficial mutations collected by the ancestral population on the trajectory toward its final phenotype, the so-called low-hanging fruit (Lenski 2017) of the adaptive process.

Though our data leave open the precise mechanism for these benefits, we propose that *S. cerevisiae* mitotypes produce extra energy and metabolites (Malecki et al. 2020) during thermal stress via enhanced respiration, relative to the putative ancestral behaviors of mitochondria from *S. paradoxus*. If so, an excess of basic building blocks would support the capacity of *S. cerevisiae* nuclear genes to confer their effects—those we study here govern housekeeping functions, namely cell division and transcription/translation. Indeed, evidence for epistasis between mitochondrial and nuclear genomes is rife in non-adaptive contexts, including reproductive barriers and aging and disease (Ellison and Burton 2008; Arnqvist et al. 2010; Tranah 2011; Joseph et al. 2013; Lovell et al. 2015; Roux et al. 2016; Loewen and Ganetzky 2018; Wolters et al. 2018; Sujkowski et al. 2019; Nguyen et al. 2020; Bushel et al. 2022; Biot-Pelletier et al. 2023; Nguyen et al. 2023; Ibrahim et al. 2024 Sep 3). For *S. cerevisiae* thermotolerance, the emerging model from our work and that of others is that evolution can use mitonuclear interactions for gains of function, as traits are built from variants in both genome compartments.

Likewise, the growth defects we have seen by cybrids at lower temperatures dovetail with results from studies of *S. cerevisiae* nuclear thermotolerance loci and those using interspecies backgrounds (Baker et al. 2019; Li et al. 2019; Hewitt et al. 2020; AlZaben et al. 2021). As a general rule, evolutionary tradeoffs are routine in the adaptation literature, from prokaryotes (Abram et al. 2021; Backman et al. 2024; Dalldorf et al. 2024) to animals (Ou et al. 2020; Ackermans 2023; Metzler et al. 2023) and plants (Gao et al. 2022; He et al. 2022; Kurepa and Smalle 2023). For yeast in particular, the exact mechanism of antagonistic pleiotropy exhibited by thermotolerance loci in cooler conditions remains unclear. Exciting recent work has revealed that *S. cerevisiae* proteins, including those encoded by mitochondria, are more thermostable than those of sister species, establishing the likely biochemical underpinning of the trait (Walunjkar et al. 2024). But it may not follow that the *S. cerevisiae* alleles of the loci we study here compromise protein structure *per se* at low temperatures (Yang et al. 2015; Cui et al. 2024). Amino acid changes unique to *S. cerevisiae* could well have tuned the temperature optima of many enzymes, as appears to be the case for the thermotolerance gene *DYN1* (Hong et al. 2016). Further work will be required to pinpoint exactly what biochemical functionality *S. cerevisiae* gave up as it acquired pro-thermotolerance alleles. Even as they stand, however, the genetics of this system help tell a story of a complex balancing act by evolution along the *S. cerevisiae* lineage, as nuclear and mitochondrial variants worked together to convert a thermosensitive ancestor to a high-temperature specialist.

Deta availability statement

The authors affirm that all data necessary for confirming the conclusion of the article are present within the article, figures, and tables. Strains are available upon request.

Acknowledgements

The authors thank members of the Brem lab, Nick Hoeffner (Stanford University), and Jun-Yi Leu (Academia Sinica, Taiwan) for experimental support and helpful discussions. This work was supported by NIH 2R01GM120430 to R.B.B.

Conflicts of interest

No conflicts of interest.

Figure captions

Figure 1. Experimental design and isolates for genetic dissection of *Saccharomyces* species variation in thermotolerance. (A) Wild-type Z1 *S. paradoxus* (purple) is used as the background for a cybrid (right) harboring the endogenous nuclear genome (N) and the mitochondrial genome from a *S. cerevisiae* donor (orange). **(B)** Strains used in this work: Sp, *S. paradoxus* Z1; Sc1 to Sc4, *S. cerevisiae* DBVPG1373, YPS128, DBVPG6044 and Y55, respectively.

Figure 2. Condition-dependent growth and tradeoffs across *Saccharomyces* species and cybrids. (A) In the main plot, each cell reports cell density, as a mean across replicates ($n \geq 3$), after 24 hours of growth in liquid culture in the respective condition, with glucose as the carbon source unless otherwise indicated. Each column reports results from wild-type *S. paradoxus* (Sp) or an isogenic cybrid harboring the mitochondrial genome from a *S. cerevisiae* donor (Scmt) labeled as in Figure 1. Colors report row-normalized z-score. In the inset, data are as in the main figure with the addition of wild-type *S. cerevisiae* DBVPG1373 (Sc). **(B-D)** Shown are reanalyses of cell density measurements across strains from the cultures and conditions in **(A)**, with respective Spearman coefficients of -0.8, 1, and 0.67. In a given panel, each dot reports median across replicates ($n \geq 3$), and error bars report standard deviations. Strain labels are as in **(A)**. *, two-tailed Mann-Whitney $p < 0.05$. Raw cell density measurements, Spearman correlation coefficients, and statistical analyses are reported in Table S2.

Figure 3. *S. cerevisiae* mitotypes boost respiration in the *S. paradoxus* nuclear background at 39°C. In each panel, in the main plot, the *y*-axis reports measurements of the reduction of 1-(4,5-dimethylthiazol-2-yl)-3,5-diphenyltetrazolium bromide after 24 hours of growth of a given strain in liquid culture with glucose as the carbon source at one temperature, normalized to the respective measurement wild-type *S. paradoxus*. In a given column, each point reports results from one biological replicate and the bar height reports the average. The *x*-axis denotes strains: wild-type *S. paradoxus* (Sp) or cybrids the mitochondrial genome from a *S. cerevisiae* donor (Scmt) labeled as in Figure 1. In the inset, data are as in the main figure with the addition of wild-type *S. cerevisiae* DBVPG1373 (Sc). **(A),** 28°C; **(B)**, 39°C. *, one-sample, two-tailed Wilcoxon $p < 0.05$. Raw data and statistical analyses are reported in Table S2.

Figure 4. Epistasis between nuclear and mitochondrial *Saccharomyces* species variants that impact thermotolerance. Each panel reports results from wild-type *S. paradoxus* Z1 (Sp) and isogenic derivatives the mitochondrial genome from a *S. cerevisiae* donor (Scmt) labeled as in Figure 1; eight nuclear thermotolerance genes from *S. cerevisiae* DBVPG1373 (8X); or both. The *y*-axis reports cell density after 24 hours of growth in liquid culture at 39°C, with glucose as the carbon source. In a given column, transparent points report replicates ($n \geq 6$) and the bold bordered point reports their average. *, two-way ANOVA $p < 0.01$ for mito-nuclear interaction. Raw cell density measurements and statistical analyses are reported in Table S2.

Supplementary figure captions

Figure S1. Stark growth differences between *S. cerevisiae* and *S. paradoxus* at high temperature. In a given panel, the *y*-axis reports cell density after 24 hours of growth in liquid culture of a wild-type homozygous diploid *Saccharomyces* strain in one temperature condition, with glucose as the carbon source. Points reports technical replicates (n = 3) and bar heights report means. Sc1, Sc2, Sc3 and Sc4 denote *S. cerevisiae* DBVPG1373, YPS128, DBVPG6044 and Y55, respectively. Sp1, Sp2, Sp3 and Sp4 denote *S. paradoxus* KPN3828, UFRJ50816, A4 and Z1, respectively. **(A)** 28°C; **(B)** 39°C. *, two-tailed Mann-Whitney $p < 0.05$. Raw cell density measurements and statistical analyses are reported in Table S2.

Figure S2. Wild-type strain and species variation in growth on glycerol. In a given panel, each bar reports results from one wild-type *S. cerevisiae* or *S. paradoxus* strain grown in liquid culture with glycerol as the carbon source from (Warringer et al. 2011). The *y*-axis reports relative growth rate **(A)** and efficiency **(B)**. *, two-talied Mann-Whitney $p < 0.05$.

Figure S3. Chronic 39°C treatment is lethal to *S. paradoxus* and to its cybrids. Shown are results of plating of the indicated strains after 24 hours of culture in one temperature condition, with glucose as the carbon source, followed by incubation of plates at 28°C for two days. Strains were wild-type *S. cerevisiae* (Sc), wild-type *S. paradoxus* (Sp), or a cybrid in the *S. paradoxus* background harboring the mitochondrial genome from a *S. cerevisiae* donor (Scmt) labeled as in Figure 1 of the main text. Raw cell density measurements and statistical analyses are reported in Table S2.

Figure S4. No detectable epistasis between nuclear and mitochondrial *Saccharomyces* species variants that impact 28°C growth. Labels are as in Figure 4. The *y*-axis reports cell density after 24 hours of growth in liquid culture at 28°C, with glucose as the carbon source. In a given column, transparent points report replicates ($n \geq 6$) and the bold bordered point reports their average. ns, two-way ANOVA $p > 0.05$ for mito-nuclear interaction. Raw cell density measurements and statistical analyses are reported in Table S2.

Figure S5. Chronic 39°C treatment is lethal to *S. paradoxus* harboring *S. cerevisiae* nuclear thermotolerance loci and to its cybrids. Labels are as in **Figure S3** except that the strains were wild-type *S. cerevisiae* (Sc), wild-type *S. paradoxus* (Sp), *S. paradoxus* harboring eight nuclear loci from *S. cerevisiae* (8X), or a cybrid in the 8X background harboring the mitochondrial genome from a *S. cerevisiae* donor (Scmt) labeled as in Figure 1 of the main text. Raw cell density measurements and statistical analyses are reported in Table S2.

352 ## Supplementary table captions

353 **Table S1. Strains used in this work.**

354 **Table S2. Growth data and statistics.** D1373, YPS128, D6044 and Y55 indicate *S. cerevisiae*
355 strains DBVPG1373, YPS128, DBVPG6044 and Y55, respectively; Sp, *S. paradoxus* Z1. The
356 first sheet contains all OD_{600} measurements of each strain at 39°C in standard glucose medium.
357 The second sheet reports the statistical analysis of the OD_{600} measurements of the cybrids at
358 39°C compared to wild-type *S. paradoxus* or the *S. paradoxus* harboring *S. cerevisiae* nuclear
359 loci (8X) by Mann-Whitney U test. The third sheet contains all OD_{600} measurements of each
360 strain at 28°C in standard glucose medium. The fourth sheet contains all OD_{600} measurements
361 of each strain at 28°C in medium with glycerol as a carbon source. The fifth sheet contains all
362 OD_{600} measurements of each strain at 28°C in medium with ethanol as a carbon source. The
363 sixth sheet contains all OD_{600} measurements of each strain at 23°C in standard glucose
364 medium. The seventh sheet reports the *p*-values of two-way ANOVA of the impact of the
365 interaction between *S. cerevisiae* mitotypes and the 8 *S. cerevisiae* loci in the *S. paradoxus*
366 background on high temperature growth (Figure 4). The eighth sheet reports the raw readouts
367 of the MTT assay at 28°C and 39°C. The ninth sheet reports the *p*-values of the normalized
368 MTT measurements by one-sample Wilcoxon with a hypothesized value of 1. The tenth sheet
369 reports the Spearman correlation coefficients and respective *p*-values of Figures 2B, 2C and
370 2D. The eleventh sheet reports the OD_{600} measurements of wild-type *S. cerevisiae* and *S.*
371 *paradoxus* strains at 28°C and 39°C in standard glucose medium with the statistical analysis
372 (Figure S1). The twelfth sheet reports the *p*-values of glycerol growth efficiency and rate of the
373 wild-type *S. cerevisiae* and *S. paradoxus* strains by two-tailed Mann-Whitney U test (Warringer
374 et al. 2011).

375

376

References

Abram F, Arcari T, Guerreiro D, O'Byrne CP. 2021. Evolutionary trade-offs between growth and survival: The delicate balance between reproductive success and longevity in bacteria. In: Advances in Microbial Physiology. Vol. 79. Elsevier. p. 133–162. https://linkinghub.elsevier.com/retrieve/pii/S006529112100014X.

Abrams MB, Dubin CA, AlZaben F, Bravo J, Joubert PM, Weiss CV, Brem RB. 2021. Population and comparative genetics of thermotolerance divergence between yeast species. G3. 11(7):jkab139. doi:10.1093/g3journal/jkab139.

Ackermans NL. 2023. Neurobiological tradeoffs of headbutting bovids. Trends in Neurosciences. 46(11):898–900. doi:10.1016/j.tins.2023.08.004.

Adhikari B, Caruso CM, Case AL. 2019. Beyond balancing selection: frequent mitochondrial recombination contributes to high-female frequencies in gynodioecious *Lobelia siphilitica* (Campanulaceae). New Phytologist. 224(3):1381–1393. doi:10.1111/nph.16136.

Allen Orr H. 2001. The genetics of species differences. Trends in Ecology & Evolution. 16(7):343–350. doi:10.1016/S0169-5347(01)02167-X.

AlZaben F, Chuong JN, Abrams MB, Brem RB. 2021. Joint effects of genes underlying a temperature specialization tradeoff in yeast. PLoS Genet. 17(9):e1009793. doi:10.1371/journal.pgen.1009793.

Amine AAA, Liao C-W, Hsu P-C, Opoc FJG, Leu J-Y. 2021. Experimental evolution improves mitochondrial genome quality control in Saccharomyces cerevisiae and extends its replicative lifespan. Current Biology. 31(16):3663-3670.e4. doi:10.1016/j.cub.2021.06.026.

Arnqvist G, Dowling DK, Eady P, Gay L, Tregenza T, Tuda M, Hosken DJ. 2010. Genetic architecture of metabolic rate: environment specific epistasis between mitochondrial and nuclear genes in an insect. Evolution. 64(12):3354–3363. doi:10.1111/j.1558-5646.2010.01135.x.

Backman T, Burbano HA, Karasov TL. 2024. Tradeoffs and constraints on the evolution of tailocins. Trends in Microbiology. 32(11):1084–1095. doi:10.1016/j.tim.2024.04.001.

Baker EP, Peris D, Moriarty RV, Li XC, Fay JC, Hittinger CT. 2019. Mitochondrial DNA and temperature tolerance in lager yeasts. Sci Adv. 5(1):eaav1869. doi:10.1126/sciadv.aav1869.

Bazzicalupo A. 2022. Local adaptation in fungi. FEMS Microbiology Reviews. 46(6):fuac026. doi:10.1093/femsre/fuac026.

Bergero R, Levsen N, Wolff K, Charlesworth D. 2019. Arms races with mitochondrial genome soft sweeps in a gynodioecious plant, Plantago lanceolata. :78254 bytes. doi:10.5061/DRYAD.TH757VG. https://datadryad.org/dataset/doi:10.5061/dryad.th757vg.

Biot-Pelletier D, Bettinazzi S, Gagnon-Arsenault I, Dubé AK, Bédard C, Nguyen THM, Fiumera HL, Breton S, Landry CR. 2023. Evolutionary Trajectories are Contingent on Mitonuclear Interactions. Molecular Biology and Evolution. 40(4):msad061. doi:10.1093/molbev/msad061.

413 Bozdag GO, Ono J, Denton JA, Karakoc E, Hunter N, Leu J-Y, Greig D. 2021. Breaking a
414 species barrier by enabling hybrid recombination. Current Biology. 31(4):R180–R181.
415 doi:10.1016/j.cub.2020.12.038.

416 Brand JA, Garcia-Gonzalez F, Dowling DK, Wong BBM. 2024. Mitochondrial genetic variation as
417 a potential mediator of intraspecific behavioural diversity. Trends in Ecology & Evolution.
418 39(2):199–212. doi:10.1016/j.tree.2023.09.009.

419 Bushel PR, Ward J, Burkholder A, Li J, Anchang B. 2022. Mitochondrial-nuclear epistasis
420 underlying phenotypic variation in breast cancer pathology. Sci Rep. 12(1):1393.
421 doi:10.1038/s41598-022-05148-4.

422 Cao Y, Vergnes L, Wang Y-C, Pan C, Chella Krishnan K, Moore TM, Rosa-Garrido M, Kimball
423 TH, Zhou Z, Charugundla S, et al. 2022. Sex differences in heart mitochondria regulate diastolic
424 dysfunction. Nat Commun. 13(1):3850. doi:10.1038/s41467-022-31544-5.

425 Chou J-Y, Hung Y-S, Lin K-H, Lee H-Y, Leu J-Y. 2010. Multiple Molecular Mechanisms Cause
426 Reproductive Isolation between Three Yeast Species. PLoS Biol. 8(7):e1000432.
427 doi:10.1371/journal.pbio.1000432.

428 Chou J-Y, Leu J-Y. 2015. The Red Queen in mitochondria: cyto-nuclear co-evolution, hybrid
429 breakdown and human disease. Front Genet. 6. doi:10.3389/fgene.2015.00187.
430 http://www.frontiersin.org/Evolutionary_and_Population_Genetics/10.3389/fgene.2015.00187/ab
431 stract.

432 Crandall JG, Fisher KJ, Sato TK, Hittinger CT. 2023. Ploidy evolution in a wild yeast is linked to
433 an interaction between cell type and metabolism. PLoS Biol. 21(11):e3001909.
434 doi:10.1371/journal.pbio.3001909.

435 Cubillos FA, Louis EJ, Liti G. 2009. Generation of a large set of genetically tractable haploid and
436 diploid *Saccharomyces* strains. FEMS Yeast Research. 9(8):1217–1225. doi:10.1111/j.1567-
437 1364.2009.00583.x.

438 Cui S, Furukawa R, Akanuma S. 2024. Insights into the low-temperature adaptation of an
439 enzyme as studied through ancestral sequence reconstruction. doi:10.1101/2024.09.05.611558.
440 http://biorxiv.org/lookup/doi/10.1101/2024.09.05.611558.

441 Dalldorf C, Rychel K, Szubin R, Hefner Y, Patel A, Zielinski DC, Palsson BO. 2024. The
442 hallmarks of a tradeoff in transcriptomes that balances stress and growth functions. mSystems.
443 9(7):e00305-24. doi:10.1128/msystems.00305-24.

444 De Chiara M, Friedrich A, Barré B, Breitenbach M, Schacherer J, Liti G. 2020. Discordant
445 evolution of mitochondrial and nuclear yeast genomes at population level. BMC Biol. 18(1):49.
446 doi:10.1186/s12915-020-00786-4.

447 Dubrovina AS, Kiselev KV. 2016. Age-associated alterations in the somatic mutation and DNA
448 methylation levels in plants. Plant Biol J. 18(2):185–196. doi:10.1111/plb.12375.

449 Elena SF. 2017. Local adaptation of plant viruses: lessons from experimental evolution.
450 Molecular Ecology. 26(7):1711–1719. doi:10.1111/mec.13836.

Ellison CK, Burton RS. 2008. Genotype-dependent variation of mitochondrial transcriptional profiles in interpopulation hybrids. Proc Natl Acad Sci USA. 105(41):15831–15836. doi:10.1073/pnas.0804253105.

Ferreira T, Rodriguez S. 2024. Mitochondrial DNA: Inherent Complexities Relevant to Genetic Analyses. Genes. 15(5):617. doi:10.3390/genes15050617.

Forejt J, Jansa P. 2023. Meiotic Recognition of Evolutionarily Diverged Homologs: Chromosomal Hybrid Sterility Revisited. Molecular Biology and Evolution. 40(4):msad083. doi:10.1093/molbev/msad083.

Fredericks LR, Lee MD, Crabtree AM, Boyer JM, Kizer EA, Taggart NT, Roslund CR, Hunter SS, Kennedy CB, Willmore CG, et al. 2021. The Species-Specific Acquisition and Diversification of a K1-like Family of Killer Toxins in Budding Yeasts of the Saccharomycotina. PLoS Genet. 17(2):e1009341. doi:10.1371/journal.pgen.1009341.

Gao H, Cui J, Liu S, Wang S, Lian Y, Bai Y, Zhu T, Wu H, Wang Y, Yang S, et al. 2022. Natural variations of ZmSRO1d modulate the trade-off between drought resistance and yield by affecting ZmRBOHC-mediated stomatal ROS production in maize. Molecular Plant. 15(10):1558–1574. doi:10.1016/j.molp.2022.08.009.

Gonçalves P, Valério E, Correia C, De Almeida JMGCF, Sampaio JP. 2011. Evidence for Divergent Evolution of Growth Temperature Preference in Sympatric Saccharomyces Species. PLoS ONE. 6(6):e20739. doi:10.1371/journal.pone.0020739.

He Z, Webster S, He SY. 2022. Growth–defense trade-offs in plants. Current Biology. 32(12):R634–R639. doi:10.1016/j.cub.2022.04.070.

Hénault M, Marsit S, Charron G, Landry CR. 2022. Hybridization drives mitochondrial DNA degeneration and metabolic shift in a species with biparental mitochondrial inheritance. Genome Res. 32(11–12):2043–2056. doi:10.1101/gr.276885.122.

Hewitt SK, Duangrattanalert K, Burgis T, Zeef LAH, Naseeb S, Delneri D. 2020. Plasticity of Mitochondrial DNA Inheritance and its Impact on Nuclear Gene Transcription in Yeast Hybrids. Microorganisms. 8(4):494. doi:10.3390/microorganisms8040494.

Hoffman GA, Garrison TR, Dohlman HG. 2002. Analysis of RGS Proteins in Saccharomyces cerevisiae. In: Methods in Enzymology. Vol. 344. Elsevier. p. 617–631. https://linkinghub.elsevier.com/retrieve/pii/S0076687902447441.

Hong W, Takshak A, Osunbayo O, Kunwar A, Vershinin M. 2016. The Effect of Temperature on Microtubule-Based Transport by Cytoplasmic Dynein and Kinesin-1 Motors. Biophysical Journal. 111(6):1287–1294. doi:10.1016/j.bpj.2016.08.006.

Hou J, Friedrich A, de Montigny J, Schacherer J. 2014. Chromosomal Rearrangements as a Major Mechanism in the Onset of Reproductive Isolation in Saccharomyces cerevisiae. Current Biology. 24(10):1153–1159. doi:10.1016/j.cub.2014.03.063.

Houtkooper RH, Mouchiroud L, Ryu D, Moullan N, Katsyuba E, Knott G, Williams RW, Auwerx J. 2013. Mitonuclear protein imbalance as a conserved longevity mechanism. Nature. 497(7450):451–457. doi:10.1038/nature12188.

490 Ibrahim R, Bahilo Martinez M, Dobson AJ. 2024 Sep 3. Rapamycin's lifespan effect is
491 modulated by mito-nuclear epistasis in *Drosophila*. Aging Cell.:e14328. doi:10.1111/acel.14328.

492 Jain AK, Singh D, Dubey K, Maurya R, Mittal S, Pandey AK. 2018. Models and Methods for In
493 Vitro Toxicity. In: In Vitro Toxicology. Elsevier. p. 45–65.
494 https://linkinghub.elsevier.com/retrieve/pii/B9780128046678000031.

495 Jhuang H, Lee H, Leu J. 2017. Mitochondrial–nuclear co-evolution leads to hybrid
496 incompatibility through pentatricopeptide repeat proteins. EMBO Reports. 18(1):87–101.
497 doi:10.15252/embr.201643311.

498 Jo YD, Lee H-Y, Ro N-Y, Kim SH, Kim J-B, Kang B-C, Kang S-Y. 2019. Mitotypes Based on
499 Structural Variation of Mitochondrial Genomes Imply Relationships With Morphological
500 Phenotypes and Cytoplasmic Male Sterility in Peppers. Front Plant Sci. 10:1343.
501 doi:10.3389/fpls.2019.01343.

502 Joseph B, Corwin JA, Li B, Atwell S, Kliebenstein DJ. 2013. Cytoplasmic genetic variation and
503 extensive cytonuclear interactions influence natural variation in the metabolome. eLife.
504 2:e00776. doi:10.7554/eLife.00776.

505 Kellis M, Patterson N, Endrizzi M, Birren B, Lander ES. 2003. Sequencing and comparison of
506 yeast species to identify genes and regulatory elements. Nature. 423(6937):241–254.
507 doi:10.1038/nature01644.

508 Kraemer SA, Boynton PJ. 2017. Evidence for microbial local adaptation in nature. Molecular
509 Ecology. 26(7):1860–1876. doi:10.1111/mec.13958.

510 Kurepa J, Smalle JA. 2023. Plant Hormone Modularity and the Survival-Reproduction Trade-Off.
511 Biology. 12(8):1143. doi:10.3390/biology12081143.

512 Leducq J-B, Henault M, Charron G, Nielly-Thibault L, Terrat Y, Fiumera HL, Shapiro BJ, Landry
513 CR. 2017. Mitochondrial Recombination and Introgression during Speciation by Hybridization.
514 Molecular Biology and Evolution. 34(8):1947–1959. doi:10.1093/molbev/msx139.

515 Lee H-Y, Chou J-Y, Cheong L, Chang N-H, Yang S-Y, Leu J-Y. 2008. Incompatibility of Nuclear
516 and Mitochondrial Genomes Causes Hybrid Sterility between Two Yeast Species. Cell.
517 135(6):1065–1073. doi:10.1016/j.cell.2008.10.047.

518 Lenski RE. 2017. Experimental evolution and the dynamics of adaptation and genome evolution
519 in microbial populations. The ISME Journal. 11(10):2181–2194. doi:10.1038/ismej.2017.69.

520 Li XC, Peris D, Hittinger CT, Sia EA, Fay JC. 2019. Mitochondria-encoded genes contribute to
521 evolution of heat and cold tolerance in yeast. Sci Adv. 5(1):eaav1848.
522 doi:10.1126/sciadv.aav1848.

523 Liao S, Chen L, Song Z, He H. 2022. The fate of damaged mitochondrial DNA in the cell.
524 Biochimica et Biophysica Acta (BBA) - Molecular Cell Research. 1869(5):119233.
525 doi:10.1016/j.bbamcr.2022.119233.

Liti G, Carter DM, Moses AM, Warringer J, Parts L, James SA, Davey RP, Roberts IN, Burt A, Koufopanou V, et al. 2009. Population genomics of domestic and wild yeasts. Nature. 458(7236):337–341. doi:10.1038/nature07743.

Loewen CA, Ganetzky B. 2018. Mito-Nuclear Interactions Affecting Lifespan and Neurodegeneration in a *Drosophila* Model of Leigh Syndrome. Genetics. 208(4):1535–1552. doi:10.1534/genetics.118.300818.

Lovell JT, Mullen JL, Lowry DB, Awole K, Richards JH, Sen S, Verslues PE, Juenger TE, McKay JK. 2015. Exploiting Differential Gene Expression and Epistasis to Discover Candidate Genes for Drought-Associated QTLs in *Arabidopsis thaliana*. Plant Cell. 27(4):969–983. doi:10.1105/tpc.15.00122.

Lupo O, Krieger G, Jonas F, Barkai N. 2021. Accumulation of *cis* - and *trans* -regulatory variations is associated with phenotypic divergence of a complex trait between yeast species. G3 Genes|Genomes|Genetics. 11(2):jkab016. doi:10.1093/g3journal/jkab016.

Malecki M, Kamrad S, Ralser M, Bähler J. 2020. Mitochondrial respiration is required to provide amino acids during fermentative proliferation of fission yeast. EMBO Reports. 21(11):e50845. doi:10.15252/embr.202050845.

Mário Š, Poláková S, Jatzová K, Sulo P. 2015. Post-zygotic sterility and cytonuclear compatibility limits in S. cerevisiae xenomitochondrial cybrids. Front Genet. 5. doi:10.3389/fgene.2014.00454. http://journal.frontiersin.org/article/10.3389/fgene.2014.00454/abstract.

Marsit S, Hénault M, Charron G, Fijarczyk A, Landry CR. 2021. The neutral rate of whole-genome duplication varies among yeast species and their hybrids. Nat Commun. 12(1):3126. doi:10.1038/s41467-021-23231-8.

Melvin RG, Ballard JWO. 2006. Intraspecific variation in survival and mitochondrial oxidative phosphorylation in wild-caught *Drosophila simulans*. Aging Cell. 5(3):225–233. doi:10.1111/j.1474-9726.2006.00211.x.

Meng X, Li L, Pascual J, Rahikainen M, Yi C, Jost R, He C, Fournier-Level A, Borevitz J, Kangasjärvi S, et al. 2022. GWAS on multiple traits identifies mitochondrial ACONITASE3 as important for acclimation to submergence stress. Plant Physiology. 188(4):2039–2058. doi:10.1093/plphys/kiac011.

Metzler S, Kirchner J, Grasse AV, Cremer S. 2023. Trade-offs between immunity and competitive ability in fighting ant males. BMC Ecol Evo. 23(1):37. doi:10.1186/s12862-023-02137-7.

Moran BM, Payne CY, Powell DL, Iverson ENK, Donny AE, Banerjee SM, Langdon QK, Gunn TR, Rodriguez-Soto RA, Madero A, et al. 2024. A lethal mitonuclear incompatibility in complex I of natural hybrids. Nature. 626(7997):119–127. doi:10.1038/s41586-023-06895-8.

Nelson ED, Grishin NV. 2018. Inference of epistatic effects in a key mitochondrial protein. Phys Rev E. 97(6):062404. doi:10.1103/PhysRevE.97.062404.

564 Nguyen THM, Sondhi S, Ziesel A, Paliwal S, Fiumera HL. 2020. Mitochondrial-nuclear
565 coadaptation revealed through mtDNA replacements in Saccharomyces cerevisiae. BMC Evol
566 Biol. 20(1):128. doi:10.1186/s12862-020-01685-6.

567 Nguyen THM, Tinz-Burdick A, Lenhardt M, Geertz M, Ramirez F, Schwartz M, Toledano M,
568 Bonney B, Gaebler B, Liu W, et al. 2023. Mapping mitonuclear epistasis using a novel
569 recombinant yeast population. PLoS Genet. 19(3):e1010401.
570 doi:10.1371/journal.pgen.1010401.

571 Nikolov LA, Tsiantis M. 2015. Interspecies Gene Transfer as a Method for Understanding the
572 Genetic Basis for Evolutionary Change: Progress, Pitfalls, and Prospects. Front Plant Sci.
573 6:1135. doi:10.3389/fpls.2015.01135.

574 Oppong RF, Terracciano A, Picard M, Qian Y, Butler TJ, Tanaka T, Moore AZ, Simonsick EM,
575 Opsahl-Ong K, Coletta C, et al. 2022. Personality traits are consistently associated with blood
576 mitochondrial DNA copy number estimated from genome sequences in two genetic cohort
577 studies. eLife. 11:e77806. doi:10.7554/eLife.77806.

578 Ou Q, Vannier J, Yang X, Chen A, Mai H, Shu D, Han J, Fu D, Wang R, Mayer G. 2020.
579 Evolutionary trade-off in reproduction of Cambrian arthropods. Sci Adv. 6(18):eaaz3376.
580 doi:10.1126/sciadv.aaz3376.

581 Paget CM, Schwartz J-M, Delneri D. 2014. Environmental systems biology of cold-tolerant
582 phenotype in Saccharomyces species adapted to grow at different temperatures. Mol Ecol.
583 23(21):5241–5257. doi:10.1111/mec.12930.

584 Pakendorf B, Stoneking M. 2005. MITOCHONDRIAL DNA AND HUMAN EVOLUTION. Annu
585 Rev Genom Hum Genet. 6(1):165–183. doi:10.1146/annurev.genom.6.080604.162249.

586 Parra M, Libkind D, Hittinger CT, Álvarez L, Bellora N. 2023. Assembly and comparative
587 genome analysis of a Patagonian *Aureobasidium pullulans* isolate reveals unexpected
588 intraspecific variation. Yeast. 40(5–6):197–213. doi:10.1002/yea.3853.

589 Peng L, Wang B, Ren P. 2005. Reduction of MTT by flavonoids in the absence of cells. Colloids
590 and Surfaces B: Biointerfaces. 45(2):108–111. doi:10.1016/j.colsurfb.2005.07.014.

591 Peris D, Ubbelohde EJ, Kuang MC, Kominek J, Langdon QK, Adams M, Koshalek JA, Hulfachor
592 AB, Opulente DA, Hall DJ, et al. 2023. Macroevolutionary diversity of traits and genomes in the
593 model yeast genus Saccharomyces. Nat Commun. 14(1):690. doi:10.1038/s41467-023-36139-
594 2.

595 Pinto J, Balarezo-Cisneros LN, Delneri D. 2025. Exploring adaptation routes to cold
596 temperatures in the Saccharomyces genus. PLoS Genet. 21(2):e1011199.
597 doi:10.1371/journal.pgen.1011199.

598 Piskur J, Rozpedowska E, Polakova S, Merico A, Compagno C. 2006. How did Saccharomyces
599 evolve to become a good brewer? Trends in Genetics. 22(4):183–186.
600 doi:10.1016/j.tig.2006.02.002.

601 Quéméneur J-B, Danion M, Cabon J, Collet S, Zambonino-Infante J-L, Salin K. 2022. The
602 relationships between growth rate and mitochondrial metabolism varies over time. Sci Rep.
603 12(1):16066. doi:10.1038/s41598-022-20428-9.

604 Rees JS, Castellano S, Andrés AM. 2020. The Genomics of Human Local Adaptation. Trends in
605 Genetics. 36(6):415–428. doi:10.1016/j.tig.2020.03.006.

606 Reuß O, Vik Å, Kolter R, Morschhäuser J. 2004. The SAT1 flipper, an optimized tool for gene
607 disruption in Candida albicans. Gene. 341:119–127. doi:10.1016/j.gene.2004.06.021.

608 Rikhvanov EG, Varakina NN, Rusaleva TM, Rachenko EI, Kiseleva VA, Voinikov VK. 2001. [No
609 title found]. Microbiology. 70(4):462–465. doi:10.1023/A:1010442429489.

610 Roop JI, Chang KC, Brem RB. 2016. Polygenic evolution of a sugar specialization trade-off in
611 yeast. Nature. 530(7590):336–339. doi:10.1038/nature16938.

612 Roux F, Mary-Huard T, Barillot E, Wenes E, Botran L, Durand S, Villoutreix R, Martin-Magniette
613 M-L, Camilleri C, Budar F. 2016. Cytonuclear interactions affect adaptive traits of the annual
614 plant *Arabidopsis thaliana* in the field. Proc Natl Acad Sci USA. 113(13):3687–3692.
615 doi:10.1073/pnas.1520687113.

616 Salvadó Z, Arroyo-López FN, Guillamón JM, Salazar G, Querol A, Barrio E. 2011. Temperature
617 Adaptation Markedly Determines Evolution within the Genus *Saccharomyces*. Appl Environ
618 Microbiol. 77(7):2292–2302. doi:10.1128/AEM.01861-10.

619 Sánchez NS, Königsberg M. 2006. Using yeast to easily determine mitochondrial functionality
620 with 1-(4,5-dimethylthiazol-2-yl)-3,5-diphenyltetrazolium bromide (MTT) assay. Biochem
621 Molecular Bio Educ. 34(3):209–212. doi:10.1002/bmb.2006.49403403209.

622 Serrano IM, Hirose M, Valentine CC, Roesner S, Schmidt E, Pratt G, Williams L, Salk J, Ibrahim
623 S, Sudmant PH. 2024. Mitochondrial haplotype and mito-nuclear matching drive somatic
624 mutation and selection throughout ageing. Nat Ecol Evol. 8(5):1021–1034. doi:10.1038/s41559-
625 024-02338-3.

626 Shoemaker M, Cohen I, Campbell M. 2004. Reduction of MTT by aqueous herbal extracts in the
627 absence of cells. Journal of Ethnopharmacology. 93(2–3):381–384.
628 doi:10.1016/j.jep.2004.04.011.

629 Slater TF, Sawyer B, Sträuli U. 1963. Studies on succinate-tetrazolium reductase systems.
630 Biochimica et Biophysica Acta. 77:383–393. doi:10.1016/0006-3002(63)90513-4.

631 Smukowski Heil C, Patterson K, Hickey AS-M, Alcantara E, Dunham MJ. 2021. Transposable
632 Element Mobilization in Interspecific Yeast Hybrids. Genome Biology and Evolution.
633 13(3):evab033. doi:10.1093/gbe/evab033.

634 Sork VL. 2017. Genomic Studies of Local Adaptation in Natural Plant Populations. Journal of
635 Heredity. 109(1):3–15. doi:10.1093/jhered/esx091.

636 Starr TN, Thornton JW. 2016. Epistasis in protein evolution. Protein Science. 25(7):1204–1218.
637 doi:10.1002/pro.2897.

638 Stern DB, Anderson NW, Diaz JA, Lee CE. 2022. Genome-wide signatures of synergistic
639 epistasis during parallel adaptation in a Baltic Sea copepod. Nat Commun. 13(1):4024.
640 doi:10.1038/s41467-022-31622-8.

641 Sujkowski A, Spierer AN, Rajagopalan T, Bazzell B, Safdar M, Imsirovic D, Arking R, Rand DM,
642 Wessells R. 2019. Mito-nuclear interactions modify Drosophila exercise performance.
643 Mitochondrion. 47:188–205. doi:10.1016/j.mito.2018.11.005.

644 Sullivan LB, Chandel NS. 2014. Mitochondrial reactive oxygen species and cancer. Cancer
645 Metab. 2(1):17. doi:10.1186/2049-3002-2-17.

646 Sulo P, Pirek M, Oltesova A, Marinoni G, Pikur J. 2003. The efficiency of functional
647 mitochondrial replacement in species has directional character. FEMS Yeast Research. 4(1):97–
648 104. doi:10.1016/S1567-1356(03)00109-0.

649 Sun J, Duan X, Hoffmann AA, Liu Y, Garvin MR, Chen L, Hu G, Zhou J, Huang H, Xue X, et al.
650 2019. Mitochondrial variation in small brown planthoppers linked to multiple traits and probably
651 reflecting a complex evolutionary trajectory. Molecular Ecology. 28(14):3306–3323.
652 doi:10.1111/mec.15148.

653 Swamy KBS, Lee H-Y, Ladra C, Liu C-FJ, Chao J-C, Chen Y-Y, Leu J-Y. 2022. Proteotoxicity
654 caused by perturbed protein complexes underlies hybrid incompatibility in yeast. Nat Commun.
655 13(1):4394. doi:10.1038/s41467-022-32107-4.

656 Sweeney J, Kuehne H, Sniegowski P. 2004. Sympatric natural and populations have different
657 thermal growth profiles. FEMS Yeast Research. 4(4–5):521–525. doi:10.1016/S1567-
658 1356(03)00171-5.

659 Syenina A, Vijaykrishna D, Gan ES, Tan HC, Choy MM, Siriphanitchakorn T, Cheng C,
660 Vasudevan SG, Ooi EE. 2020. Positive epistasis between viral polymerase and the 3´
661 untranslated region of its genome reveals the epidemiologic fitness of dengue virus. Proc Natl
662 Acad Sci USA. 117(20):11038–11047. doi:10.1073/pnas.1919287117.

663 Tranah GJ. 2011. Mitochondrial–nuclear epistasis: Implications for human aging and longevity.
664 Ageing Research Reviews. 10(2):238–252. doi:10.1016/j.arr.2010.06.003.

665 Tsai T, St. John JC. 2016. The role of mitochondrial DNA copy number, variants, and haplotypes
666 in farm animal developmental outcome. Domestic Animal Endocrinology. 56:S133–S146.
667 doi:10.1016/j.domaniend.2016.03.005.

668 Vijayraghavan S, Kozmin SG, Strope PK, Skelly DA, Lin Z, Kennell J, Magwene PM, Dietrich
669 FS, McCusker JH. 2019. Mitochondrial Genome Variation Affects Multiple Respiration and
670 Nonrespiration Phenotypes in *Saccharomyces cerevisiae*. Genetics. 211(2):773–786.
671 doi:10.1534/genetics.118.301546.

672 Wallace DC. 2015. Mitochondrial DNA Variation in Human Radiation and Disease. Cell.
673 163(1):33–38. doi:10.1016/j.cell.2015.08.067.

674 Walunjkar N, Lai TY, Akhter N, Miller JH, Bettinger JQ, Marcus E, Phizicky EM, Ghaemmaghami
675 S, Fay JC. 2024. Pervasive divergence in protein thermostability is mediated by both structural

676 changes and cellular environments. doi:10.1101/2024.12.09.627561.
677 http://biorxiv.org/lookup/doi/10.1101/2024.12.09.627561.

678 Warringer J, Zörgö E, Cubillos FA, Zia A, Gjuvsland A, Simpson JT, Forsmark A, Durbin R,
679 Omholt SW, Louis EJ, et al. 2011. Trait Variation in Yeast Is Defined by Population History. PLoS
680 Genet. 7(6):e1002111. doi:10.1371/journal.pgen.1002111.

681 Weinreich DM, Watson RA, Chao L. 2005. Perspective: Sign epistasis and genetic constraint on
682 evolutionary trajectories. Evolution. 59(6):1165–1174.

683 Weiss CV, Brem RB. 2019. Dissecting Trait Variation across Species Barriers. Trends in
684 Ecology & Evolution. 34(12):1131–1136. doi:10.1016/j.tree.2019.07.013.

685 Weiss CV, Roop JI, Hackley RK, Chuong JN, Grigoriev IV, Arkin AP, Skerker JM, Brem RB.
686 2018. Genetic dissection of interspecific differences in yeast thermotolerance. Nat Genet.
687 50(11):1501–1504. doi:10.1038/s41588-018-0243-4.

688 Wolff JN, Ladoukakis ED, Enríquez JA, Dowling DK. 2014. Mitonuclear interactions:
689 evolutionary consequences over multiple biological scales. Philos Trans R Soc Lond B Biol Sci.
690 369(1646):20130443. doi:10.1098/rstb.2013.0443.

691 Wolters JF, Charron G, Gaspary A, Landry CR, Fiumera AC, Fiumera HL. 2018. Mitochondrial
692 Recombination Reveals Mito–Mito Epistasis in Yeast. Genetics. 209(1):307–319.
693 doi:10.1534/genetics.117.300660.

694 Wolters JF, Chiu K, Fiumera HL. 2015. Population structure of mitochondrial genomes in
695 Saccharomyces cerevisiae. BMC Genomics. 16(1):451. doi:10.1186/s12864-015-1664-4.

696 Yang L-L, Tang S-K, Huang Y, Zhi X-Y. 2015. Low Temperature Adaptation Is Not the Opposite
697 Process of High Temperature Adaptation in Terms of Changes in Amino Acid Composition.
698 Genome Biol Evol. 7(12):3426–3433. doi:10.1093/gbe/evv232.

699

700

701 # Materials and methods

702 **Strain construction**

703 Strains used in this study are listed in Table S1. For phenotyping in Figure S1, we used wild-
704 type, homozygous diploid *S. cerevisiae*, DBVPG1373, YPS128, DBVPG6044 and Y55, and *S.*
705 *paradoxus* strains, Z1, UFRJ50816, A4 and KPN3828, from the Saccharomyces Genome
706 Resequencing Project (SGRP) collection (Table S1) (Cubillos et al. 2009). To make haploid
707 strains for the recipients for *S. cerevisiae* mitochondrial DNA, we first generated prototrophic
708 versions of diploid *S. paradoxus* Z1 and the *S. paradoxus* harboring the 8 *S. cerevisiae* loci,
709 designated as 8X (AlZaben et al. 2021). For this, the *HO* loci of the diploid wild-type Z1 and 8X
710 strains were knocked out using the hygromycin resistance gene as the selection marker using
711 the transformation protocol from (Reuß et al. 2004), with selection on 200 μg/ml hygromycin and
712 PCR and sequence confirmation. The resulting *ho⊿*::Hyg diploid strains were induced to
713 sporulate essentially as in (Lee et al. 2008), and mating types of the resulting haploids were
714 checked via halo assay following the protocol in (Hoffman et al. 2002), using JRY02375 and
715 JRY02176 as the mating testers. Next, for haploid MATα *S. paradoxus* Z1 and its descendant
716 8X, we generated a petite version of each (lacking mitochondrial DNA, ρ^0), using the protocol
717 adopted from (Amine et al. 2021).

718 Finally, we used wild-type, MATα haploid, G418-resistant, hygromycin-resistant *S. cerevisiae*
719 strains (DBVPG1373, YPS128, DBVPG6044 and Y55) mitochondrial DNA from the SGRP
720 collection (Table S1) (Cubillos et al. 2009) as donors of mitochondrial DNA for cybrids in our *S.*
721 *paradoxus* wild-type and 8X backgrounds. Our method for cybrid construction used the
722 cytoduction protocol of (Nguyen et al. 2020) as follows. We first constructed a heterokaryon-
723 competent *S. cerevisiae* strain harboring each mitotype of interest, referred to as a carrier. For
724 this, a single colony of each donor in turn, and a single colony of the ρ^0 *kar1*-d15 mutant
725 (JRY5450, a generous gift from Dr. Jasper Rine), were each inoculated into a separate 3 mL of
726 liquid YPD (1% yeast extract, 2% peptone, 2% glucose) and incubated at 28°C overnight with
727 shaking at 250 rpm. We mixed 100 μL of the two, spotted on a YPD plate, and incubated at
728 28°C for 4 hours. The mixed cellular patch was inoculated into 3 mL of YPD and incubated at
729 28°C for 2 hours with shaking at 250 rpm to promote cell division. After a 2-hour incubation, 10^{-5}
730 OD_{600} of cells were spread on a YPG plate (1% yeast extract, 2% peptone, 2% glycerol) to
731 select for mitochondrial genome retention. Colonies on the YPG plates were transferred to a
732 YPD plate with 200 μg/mL hygromycin or 200 μg/mL G418 to check for hygromycin and G418
733 sensitivity; we earmarked and preserved drug-sensitive, respiration-competent strains as those
734 in which the donor mitochondrial DNA had successfully been transferred to the JRY5450
735 nuclear background. We next used each carrier strain in turn to transfer the *S. cerevisiae*
736 mitochondrial DNA of interest into the haploid *S. paradoxus* Z1 ρ^0 strain and, separately, its
737 descendant, the 8X ρ^0 strain. This cytoduction proceeded as above except that the carrier and
738 the *S. paradoxus* strain were mated and the progeny were selected on YPG alone; afterward we
739 subjected them to the halo assay, to eliminate the carrier-*S. paradoxus* diploid hybrids, and only
740 those strains that behaved as haploid MATα were retained as cybrids.

741 **Growth assays**

742 Measurements of carrying capacity at 39°C were done as described (AlZaben et al. 2021) with
743 some modifications. To make sure the cells were respiratory-competent before the assay,
744 strains were streaked on YPG plates and were allowed to grow at 28°C for 4 days to form
745 colonies. Three colonies were inoculated into 15 mL of liquid YPG and incubated at 28°C for
746 overnight with shaking at 250 rpm. The cultures would reach 0.4-0.8 OD_{600} after a 16-hour
747 growth. The cultures were then back-diluted into 5 mL of YPD, YPE (1% yeast extract, 2%

748 peptone, 2% ethanol), or YPG to achieve 0.1 OD_{600}/mL, and then incubated at 23°C, 28°C or
749 39°C for 24 hours. This procedure, from streaking on solid agar plates to biomass
750 measurement, was repeated at least twice for each strain with three technical repeats in each
751 biological replicate. We collected the readouts of carrying capacity from all the replicates across
752 all days for a given strain and compared each mitochondrial transgenic to *S. paradoxus* with a
753 two-tailed Mann-Whitney U test. For epistatic analysis, a two-way ANOVA test was carried out to
754 examine the impact of the genotype-mitotype interaction on thermotolerance. All the statistical
755 analyses were done with scipy.stats in Python 3.7.

756 **MTT assay**

757 To measure respiration efficiency, pre-culture and treatment were as in Growth assays, above,
758 and after 24 hours we carried out the MTT assay as in (Sánchez and Königsberg 2006).
759 Independent experiments from growth to MTT measurement were performed at least six times.
760 The readouts were normalized to that of wild-type *S. paradoxus* at either 28°C or 39°C. Two-
761 tailed one-sample Wilcoxon test was performed using the normalized data with a hypothesized
762 value of 1 with scipy.stats in Python 3.7.

763 **Growths of *S. cerevisiae* and *S. paradoxus* in glycerol**

764 Data are from (Liti et al. 2009) and Mann-Whitney U test was performed to compare the growths
765 of the two species in glycerol with scipy.stats in Python 3.7.

766

Fig 1

(A)

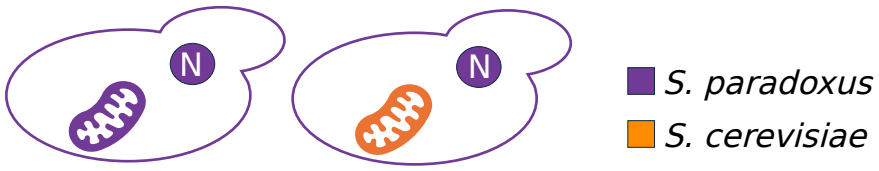
N
N
S. paradoxus
S. cerevisiae

(B)

Sp
Sc1
Sc4
Sc2
Sc3
Oak tree
Soil
Wine
Soil
Grapes

Fig 2

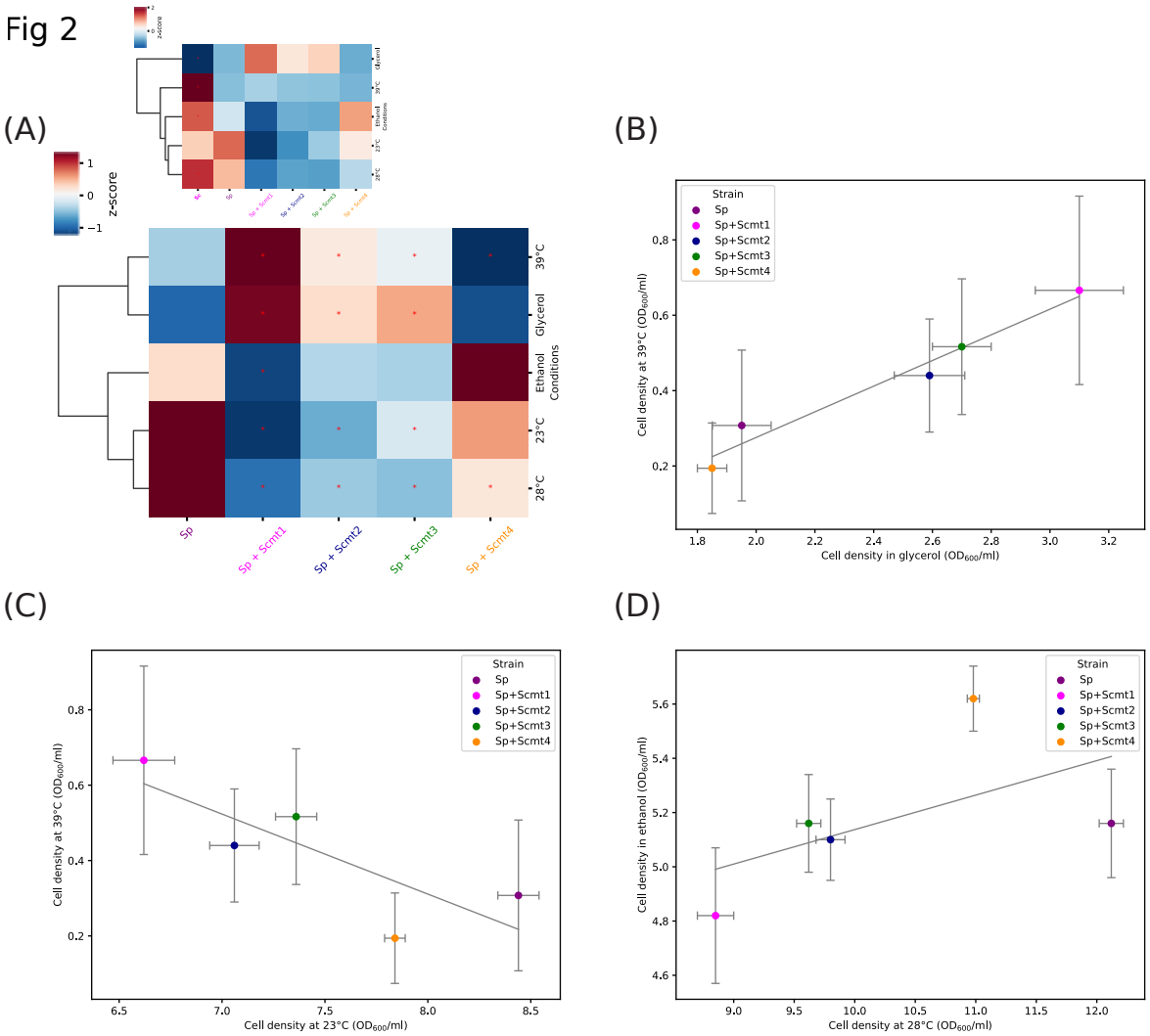
(A)
z-score
1
0
−1
39°C
Glycerol
Ethanol
Conditions
23°C
28°C
Sp
Sp + Scmt1
Sp + Scmt2
Sp + Scmt3
Sp + Scmt4
(B)
Strain
Sp
Sp+Scmt1
Sp+Scmt2
Sp+Scmt3
Sp+Scmt4
Cell density at 39°C (OD600/ml)
Cell density in glycerol (OD600/ml)
(C)
Cell density at 39°C (OD600/ml)
Cell density at 23°C (OD600/ml)
(D)
Cell density in ethanol (OD600/ml)
Cell density at 28°C (OD600/ml)

Fig 3

(A)

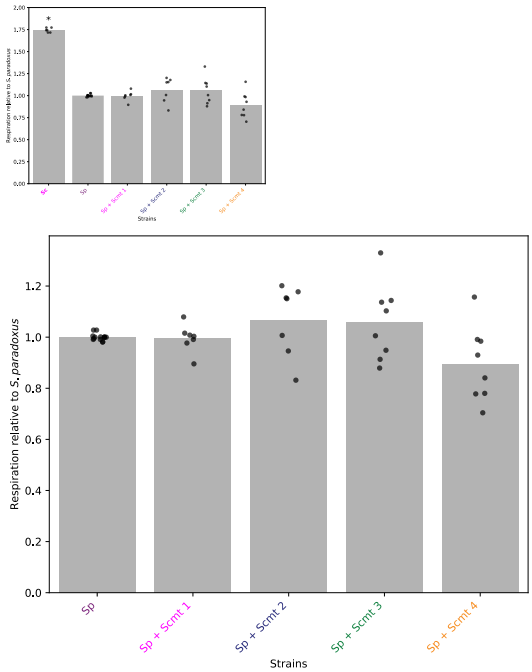
Respiration relative to S.paradoxus
Sp
Sp + Scmt 1
Sp + Scmt 2
Sp + Scmt 3
Sp + Scmt 4
Strains

(B)

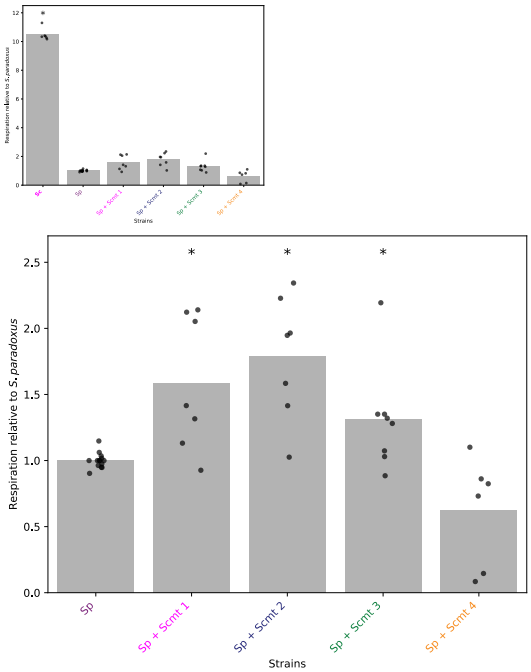
Respiration relative to S.paradoxus
*
*
*
Sp
Sp + Scmt 1
Sp + Scmt 2
Sp + Scmt 3
Sp + Scmt 4
Strains

Fig 4

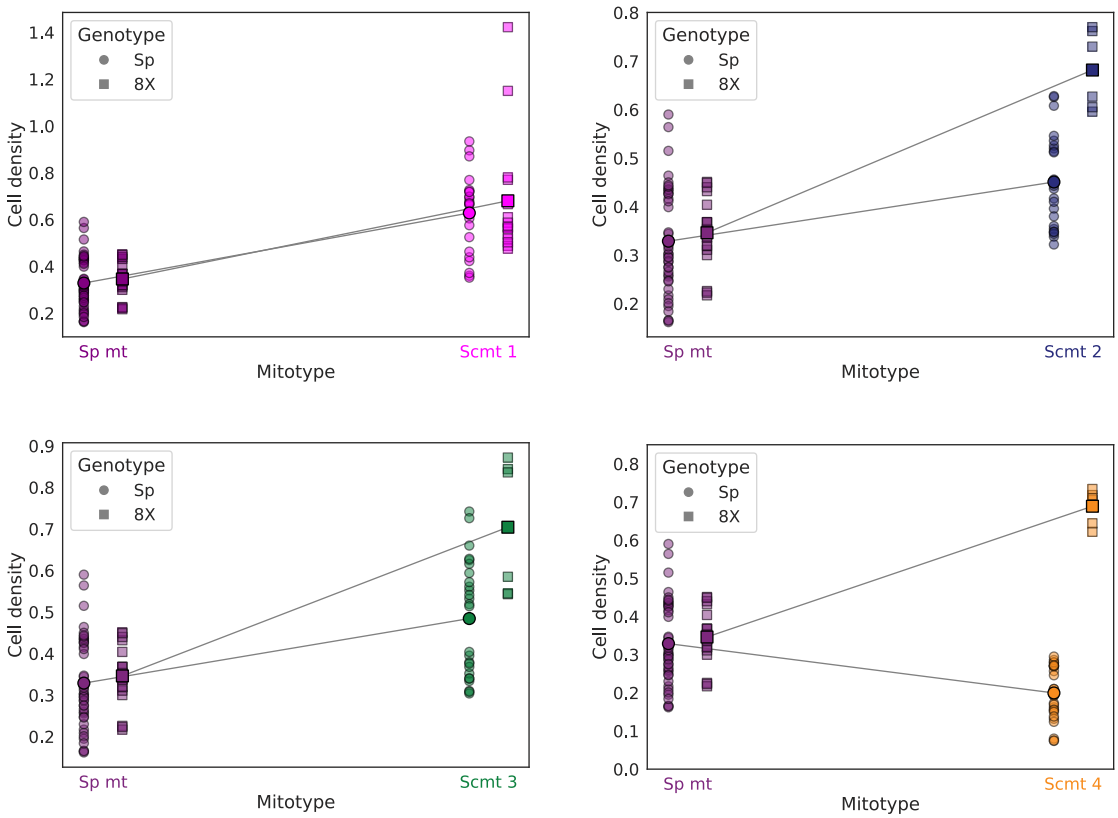
Genotype
Sp
8X
Cell density
Mitotype
Sp mt
Scmt 1
Scmt 2
Scmt 3
Scmt 4